Novel Analog Self-Electrooptic-Effect Devices

David A. B. Miller, *Senior Member, IEEE*

Abstract—**New circuits and modes of operation for quantum-well self-electrooptic-effect devices (SEED) are proposed that allow analog processing of optical images and arrays. Analog functions performed include addition, subtraction, uniform amplification, replication, spatial differentiation, convolution, cross-correlation, and optically controllable weights for matrix-vector processors or neural nets. Many of the devices can operate with differential pairs of light beams, allowing full bipolar analog processing, and other devices can convert between differential and single-beam representations. Many of the circuits could be made using the existing SEED array process. The devices should be sensitive enough to allow direct processing at video frame rates of scenes under normal room illumination. Operation up to speeds of nanoseconds is predicted for proportionately higher powers.**

I. Introduction

QUANTUM-well self-electrooptic-effect devices (SEED's) [1], [2] are a family of optoelectronic devices based on the large electroabsorptive mechanisms, such as the quantum-confined Stark effect [3], seen in such layered semiconductor structures, and on the concept of integrating photodetection with such absorption modulation. Both modulators and detectors can be made with the same structure; the modulator usually consists of a p–i–n diode with quantum-well layers in the *i*-region. This integration, and the low energies required to operate the quantum-confined Stark effect modulators, allow various novel optoelectronic devices and functions, with optical or electrical inputs and outputs. Although some analog functions have been proposed and demonstrated [4], [5], SEED's have been most extensively investigated for digital systems. The symmetric SEED (S-SEED) [6] has been particularly useful for systems experiments, in part because of many features of operating with differential pairs of light beams. Large two-dimensional (2-D) arrays of such devices have been demonstrated.

One analog SEED configuration that was successfully demonstrated was the so-called "self-linearized" modulator [4], [6]. This configuration allows a modulator to be controlled linearly by a control current or another light beam power. The present paper extends this concept to several new configurations. Some of the concepts here are "single-ended", that is, operating on light beams singly as inputs or outputs. Many of the concepts, however, operate with differential *pairs* of light beams, as inputs, outputs or both, or use *differences* in light intensities as inputs; these devices can be viewed as analog versions or extensions of the S-SEED. This differential concept opens up many new possibilities for SEED functions. The use of differential pairs allows positive and negative values to be represented and processed, and the differencing of intensities allows various spatial derivatives to be evaluated. Hence these differential ideas offer a solution to the problem of processing bipolar values in "incoherent" optical analog processing (see, e.g., [7] and [8]). They represent an alternative approach to many of these analog functions, compared to, for example, approaches with photorefractive materials [9].

The basic concepts presented here allow many different sophisticated analog functions to be performed. Functions described here include: addition, subtraction, and spatial differentiation of images; correlation; optically controlled bipolar matrix-vector multiplication (e.g., for optical neural nets); amplification of an image by an integer gain; and replication of an image (with equal powers in each replica) without beam splitters. In many cases, the devices described here can be made using the same technology as has been used successfully to make large arrays of S-SEED's. The devices should also be able to operate over a very large range of speeds and powers. These proposed devices therefore offer many new opportunities for high-performance, sophisticated, analog optical processing of images and 2-D arrays.

In this paper, we will concentrate on device configurations. We will not attempt to give complete architectures for systems, nor will we discuss optics in any detail. We will however discuss some example device configurations for various potential applications, and these do require some special optical techniques. Many of the devices are intended to work with pixelated images. There are several ways of generating these, including simple masks with holes, or lenslet arrays. Many of the schemes too require that the pixelated images be "interlaced"; pixels from two different images may be alternated with one another on the device plane. This can be achieved in a number of ways also, the simplest being a patterned mirror used as a beam splitter, reflecting the set of pixels from one array and passing the set of pixels from another array. Such techniques have been used extensively in digital systems (see, e.g., [10]), and much of the optics can be borrowed from the digital case.

The structure of this paper is as follows. In section II, we briefly summarize the concepts of self-linearized modulation, which is common to all of the devices discussed here. In Section III, we introduce the various basic dif-

Manuscript received March 15, 1992; revised August 4, 1992.
The author is with AT&T Bell Laboratories, Holmdel, NJ 07733.
IEEE Log Number 9205863.

ferential SEED circuits that are used to perform many of the differential functions, and describe how such devices could be made. In Section IV, we discuss various possible applications of the basic differential SEED circuits, including addition and subtraction, neural net nodes and optically controllable weights, spatial differentiation, and correlation. In Section V, we introduce the concepts of integer gain SEED's for amplification (stacked SEED) and replication (replicating SEED) of single-ended images or arrays. Section VI extends the integer gain concepts to the differential case, including techniques for derivatives and correlations of pixelated images. Section VII describes the expected physical performance of these devices, in terms of their speeds and operating powers and intensities. Conclusions are summarized in Section VIII. An Appendix derives the design relations for stacked SEED's.

II. Self-Linearized Modulation

To understand all of the devices discussed here, it is important to understand the concept of self-linearized modulation with a quantum-well diode. This has been discussed in detail before [4]. For completeness, we will briefly summarize the principle here. Fig. 1 shows the simplest self-linearized modulator circuit.

The p–i–n diode contains quantum wells in the *i*-region. Photons absorbed in the *i*-region generate photocarriers. In practice, such diodes can be made so that, over a wide range of reverse bias, and sometimes even partly into forward bias, essentially exactly one electron of current flows for each photon absorbed in the quantum well region, i.e.,

$$I_A = \frac{e}{\hbar\omega} P_A \tag{1}$$

where I_A is the generated photocurrent, $\hbar\omega$ is the photon energy, e is the electronic charge. The absorbed power P_A is given by

$$P_A = P_{\text{in}} - P_{\text{out}} \tag{2}$$

where P_{in} and P_{out} are the incident (input) and transmitted (output) powers, respectively, in the light beam. We assume here that there is no loss in or reflection from the n or p regions; this is reasonable since the n and p regions can readily be made from transparent semiconductors and the surfaces can be antireflection coated. The theory discussed here could be extended to cover such losses and reflections.

In such a circuit as Fig. 1 with a quantum-well diode, the absorbed power depends on the voltage across the diode because of electroabsorption mechanisms such as the quantum-confined Stark effect (QCSE). This means that, for a given input optical power, the photocurrent depends on the voltage across the diode. The photocurrent in turn will change the voltage because of the external circuit through which it passes. Hence there is a feedback mechanism. In most simple circuits, this feedback will be positive if the absorption decreases with (reverse bias)

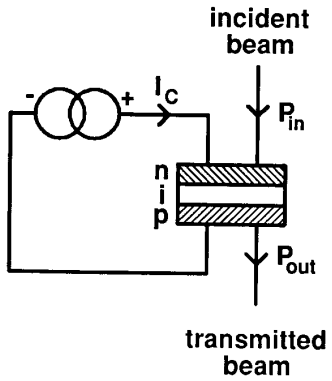

Fig. 1. Simple self-linearized modulator schematic. The p–i–n structure is a diode containing quantum wells in the *i*-region.

voltage across the diode [4]. Such positive feedback can give bistable switching into a high-absorption low-voltage state with increasing input power. Such bistability can be seen by operating at a photon energy corresponding to the zero electric field position of the exciton absorption peak. All of the circuits to be discussed here operate in the *negative* feedback mode. The photon energy is chosen to be such that the diode absorption and photocurrent *increase* with increasing voltage. Such behavior can usually be found by choosing the photon energy just below the zero field exciton peak position, because there the absorption increases with increasing voltage as the optical absorption edge shifts to lower photon energies with increasing electric field.

For the specific case of Fig. 1, with the photon energy chosen for negative feedback, the net result is that the voltage across the diode adjusts itself so that the generated photocurrent I_A is equal to the current I_C from the current generator. (A current generator is simply a source whose current output is independent of voltage, with a simple example being a very large resistor connected in series with a battery of very high voltage.) If the diode was generating too much photocurrent, there would be a net current $I_A - I_C$ that would act to discharge the capacitance of the diode, decreasing the voltage across the diode, and hence reducing the absorption of the diode. If the diode was generating too little photocurrent, the opposite would happen, increasing the voltage across the diode, and hence increasing the absorption. Hence the stable state is

$$I_A = I_C. \tag{3}$$

Consequently, we now obtain the very unusual behavior that the absorbed power is linearly proportional to the current generator current, i.e.,

$$P_A = \frac{\hbar\omega}{e} I_C. \tag{4}$$

For a given input power, the output power decreases linearly with the drive current. All that is required for linearity is that one electron of photocurrent flows for each absorbed photon. The limits of the range of linearity are

set by the maximum and minimum absorption possible for the given quantum well diode. Such self-linearized modulation has been clearly demonstrated [4].

III. Differential SEED Circuits

Some of the success of the S-SEED in digital systems was due to features of pairs of light beams. For example, since the device is switched by changing the ratio of the light beams in the pair, the absolute power in the light beams becomes relatively unimportant. Hence neither the absolute power in the beams from the light source nor the degree of attenuation between the output of one device and the input of the next is very important. This use of the ratio of two beam powers also relaxes the requirements on the uniformity of arrays of light beams used to drive arrays of such devices. It is only important that adjacent light beams be substantially equal in power. Smooth variations over a whole array of beams do not matter very much. The use of pairs of light beams also overcomes one constraint with the SEED's in practice, which is that it is difficult to obtain very large contrast of modulation in the output of the devices. A logic state "1" can be represented by beam A being more powerful than beam B, and vice versa for a logic "0". Such a representation works well even with contrasts in power of as little as 2 : 1 between the "bright" and "dark" states of the beams. For the particular case of the digital system, the use of pairs of light beams also allowed substantial gain (so-called "time-sequential" gain) without critical setting of any parameters.

Some of the features of working with pairs of light beams are also applicable to analog systems. In optics, it is simplest to represent an analog signal with a single light beam, but this causes some problems that can be difficult for practical devices. One problem is that it is difficult to represent both positive and negative values because the power in the light beam is always positive. One can exploit another degree of freedom, such as polarization or phase, to allow positive and negative values to be represented. Another option is the present one of using pairs of light beams. If beam A is more powerful than beam B, the value represented is positive; for B more powerful than A, the opposite is true. In this case, the analog value could be represented either by the difference between the two powers or by their ratio. The use of such pairs of beams also gives an infinite dynamic range in one sense even with modulators of finite contrast ratio, since we can represent values all the way down to zero, corresponding to equal beam powers.

The differential circuits described here operate on and with the difference in powers of two beams in a pair, rather than the ratio. In this case, we do not get all of the desirable features found with the ratio, although we do retain many. We do have good tolerance both to variations in the absolute power in our power supply beams and to spatial nonuniformity of light beams used to power arrays of analog devices, just as in the digital S-SEED case. As long as the two powers in a pair of supply beams are equal, their absolute magnitude will not change the size of the differential output power (and hence it will not change the differential output signal); it will only change the overall background power. If, however, we have loss between two stages in the system, the loss will reduce the magnitude of the differential signal (which it would not if we worked with the ratio of the beam powers). The ability to represent both positive and negative values, and the insensitivity to power supply fluctuations, are, none the less, very important advantages.

Use of differential pairs of light beams is relatively unusual in analog processing. Up to now, there have not been many devices suitable for this. It is also true that the optics required for working this way is more complicated, and many input signals, such as pictorial images, exist originally in unipolar form. As we will show below, however, it is not difficult to convert between the two forms using variations of the basic devices and configurations used for the differential devices and optics, provided only that we pixelate the image.

Incidentally, although here we will only illustrate the operation of the differential devices using transmission of light beams through the quantum well diodes, all of these differential devices work equally well if there is a mirror beneath the quantum-well diodes, and we work in reflection with the beam passing through the quantum-well diode, reflecting off of the mirror, and passing back through the diode. Many of the present SEED arrays are made in this way.

A. Differential Detectors

It is well known that a conventional photodiode can be designed to give a photocurrent that is substantially independent of reverse bias, depending only on the incident light power. Such a device relies on generating one electron of current for every photon absorbed. Such photodiodes, with light beams shining on them, have been used successfully as appropriate current sources for self-linearized modulators before [4], [5]. A simple extension of this is to use a pair of such photodiodes in series to act as a current source whose current value depends on the difference of the light powers shining on the two diodes. This is illustrated in Fig. 2.

We assume for simplicity for such conventional diodes that all of the incident power on a given diode gives rise to photocurrent, with one incident photon giving one electron of photocurrent. Again, the theory discussed here could be extended to cover any other constant ratio of photocurrent to incident power. In the steady state, the current I_C flowing into the circuit connected to the output will simply be the difference of the photocurrents generated in the two diodes 1 and 2, i.e.,

$$I_C = \frac{e}{\hbar\omega}(P_1 - P_2). \tag{5}$$

In Fig. 2, V_0 is a constant supply voltage. For the circuit of Fig. 2, the current I_C can be of either sign, al-

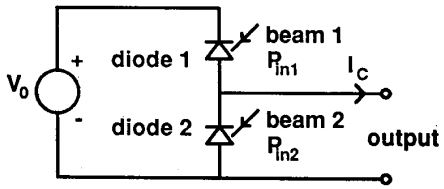

Fig. 2. Differential photodiode detectors as a constant current source.

though the voltage at the output terminals can essentially only be positive. This is not an important restriction for the applications we discuss below. This circuit will be the main optical input circuit for the differential input devices.

Connecting a single reverse biased quantum-well p–i–n diode across the output terminals as shown in Fig. 3 gives a circuit that converts a differential optical signal into a "single ended" one through the self-linearized behavior of the quantum-well diode.

From (4) and (5), we have for the output power P_{out}

$$P_{out} = P_{in} - (P_1 - P_2). \tag{6}$$

For a fixed optical "bias" P_{in}, we have therefore performed the differential-to-single-ended conversion. Of course, the circuit of Fig. 3 can only work if P_1 is greater than P_2, since the quantum-well diode must have a positive current flowing through it. This is an unavoidable consequence of converting from a differential representation back to a single-ended one, since the single-ended representation must be positive. It may be necessary to add a bias beam input to diode 1 to "level-shift" the output so that the current into the quantum-well diode is positive.

B. Differential Self-Linearized Modulators

Fig. 4 shows the circuit for a self-linearized differential modulator. In the steady state, it is clear from a simple application of conservation of current that the difference in the two photocurrents I_1 and I_2 must be equal to the source current I_C i.e.,

$$I_2 - I_1 = I_C. \tag{7}$$

Hence, the difference in the absorbed powers P_{A1} and P_{A2}, respectively, in the two quantum-well diodes is given by

$$P_{A2} - P_{A1} = \frac{\hbar\omega}{e} I_C. \tag{8}$$

This circuit therefore gives a *difference* in absorbed powers that is linearly proportional to the drive current. It is useful to express the operation of this circuit in terms of differences in beam powers. If we define the difference D_{in} in input beam powers as

$$D_{in} = P_{in1} - P_{in2} \tag{9}$$

and the difference D_{out} in output beam powers as

$$D_{out} = P_{out1} - P_{out2} \tag{10}$$

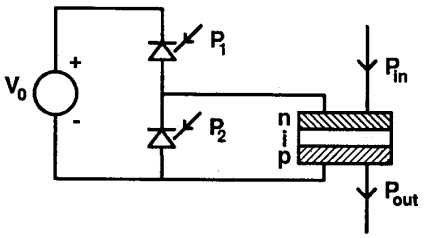

Fig. 3. Circuit for converting a differential optical signal into a single ended one.

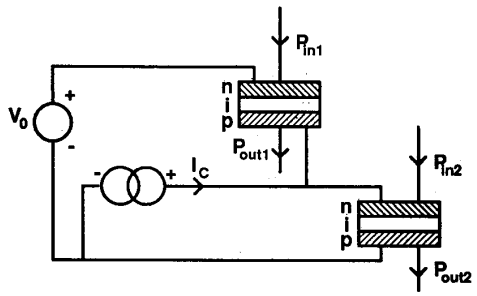

Fig. 4. Differential self-linearized modulator circuit.

then we have

$$D_{out} = D_{in} + \frac{\hbar\omega}{e} I_C. \tag{11}$$

In one simple mode of operation, the input optical bias or "power supply" beams P_{in1} and P_{in2} would have equal powers (i.e., $D_{in} = 0$). Then we would have the simple result that the difference in optical output powers was linearly proportional to the drive current.

Of course, the current source in Fig. 4 could be a reverse biased photodiode illuminated with a beam of power P_D as in Fig. 5. In this case, we would have

$$D_{out} = D_{in} + P_D \tag{12}$$

in which the change in D_{out} is the input power P_D. If the input beams P_{in1} and P_{in2} were equal (i.e., $D_{in} = 0$), we would in this case have a circuit to convert a single ended optical signal to a differential one.

Now we can combine the concepts of Figs. 4 and 2 to make a circuit with both differential inputs and differential outputs as shown in Fig. 6. In this circuit for simplicity we have used the same voltage supply for both pairs of photodiodes, although this is not a necessary restriction. Now the output power difference D_{out} is given by

$$D_{out} = D_\alpha + D_\beta \tag{13}$$

where D_α and D_β are the differences in the input powers

$$D_\alpha = P_{\alpha 1} - P_{\alpha 2} \tag{14a}$$

and

$$D_\beta = P_{\beta 1} - P_{\beta 2}. \tag{14b}$$

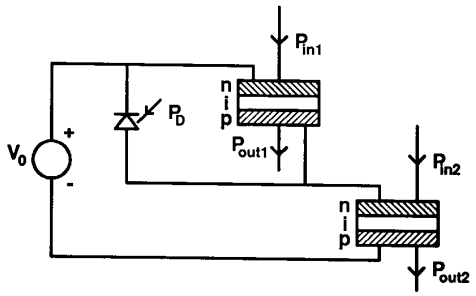

Fig. 5. Circuit for conversion of single ended optical signals to differential optical outputs.

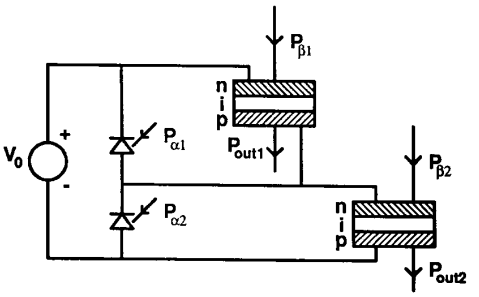

Fig. 6. Self-linearized differential light-by-light modulator. This circuit also gives a difference in output beam powers that is the sum of the differences in the two pairs of input beam powers.

In the simple case of equal bias beam powers (i.e., $D_\beta = 0$), we have a circuit that transfers the difference in two input power beams linearly to the output power beams. In the general case, the circuit adds the differences in the two sets of beams, as shown in (13).

This circuit will be used to perform various different functions that we will discuss below. One simple function of the circuits that it resets the bias level on the differential signal. For example, the overall input powers $P_{\alpha 1}$ and $P_{\alpha 2}$ could be large, but have only small differences, as in the case of two images that are similar. The large common power can be suppressed in the output by transfering the difference onto weaker beams $P_{\beta 1}$ and $P_{\beta 2}$. Another simple function is to add or subtract two differential input signals, simply by shining both of them onto the *conventional* photodiodes. We can imagine that the powers $P_{\alpha 1}$ and $P_{\alpha 2}$ are the total powers from two light beams shining on each of the conventional photodiodes, i.e.,

$$P_{\alpha 1} = P_{\gamma 1} + P_{\epsilon 1} \tag{15a}$$

and

$$P_{\alpha 2} = P_{\gamma 2} + P_{\epsilon 2}. \tag{15b}$$

It is now trivially obvious that

$$D_\alpha = D_\gamma + D_\epsilon \tag{16}$$

where D_γ and D_ϵ are the differences in input powers

$$D_\gamma = P_{\gamma 1} - P_{\gamma 2} \tag{17a}$$

and

$$D_\epsilon = P_{\epsilon 1} - P_{\epsilon 2}. \tag{17b}$$

Because of the differential representation, we can also use this circuit for subtraction simply by interchanging the beams $P_{\gamma 1}$ and $P_{\gamma 2}$ (or by interchanging the beams $P_{\epsilon 1}$ and $P_{\epsilon 2}$ depending on the sense of the subtraction desired). Equivalently, we could leave the beams physically where they are, but shine them onto two pairs of conventional photodiodes, electrically in parallel, but with the second pair rewired to interchange the roles of the two diodes. Similar addition and subtraction can be performed on the beam pairs D_α and D_β. Hence, by using such circuits in arrays, with images represented differentially in arrays, we can perform linear addition and subtraction of images; we will show example layouts of these circuits also below.

Notice that in the circuits of Figs. 4, 5, and 6, the results on the differences in the output beam powers are independent of the absolute power levels in any of the beams. Only the difference in power in any pair of beams matters. Of course, we must stay within the allowable range of absorption of the modulators, but we have removed any sensitivity to moderate changes in the absolute power levels by this differential operation.

C. Physical Structure of Devices

There are two approaches that we will discuss here for implementing arrays of the basic devices discussed above. One is to construct a special layer structure that allows both conventional and quantum-well photodiodes; this would have the most ideal performance. The second approach is to utilize the existing S-SEED process; this is easier to make, although it involves some compromises in the device performance.

1) *Structure with conventional and quantum-well diodes:* An example of a special layer structure is shown in Fig. 7. On the top of the whole structure is a "conventional" p–i–n photodiode in layers 1–3. Layers 1 and 3 would be made of transparent material (e.g., AlGaAs), and the absorbing layer, layer 2, (e.g., GaAs) would be designed sufficiently thick so as to absorb essentially all of the incident light (e.g., 1–2 μm). Optionally, a dielectric stack mirror, made of alternating quarter wavelength thick layers of two different semiconductors (e.g., AlGaAs and AlAs) could be incorporated within layers 3 and 4 so as to reflect any light not absorbed in layer 2 back into layer 2 for further absorption. Antireflection coatings could be applied to both of the exposed surfaces of layers 1 and 5 to prevent reflection off of the surface and hence improve the efficiency of absorption. Alternatively, with some restriction on operating wavelength, these surfaces could be uncoated, or even reflection coated, to form resonators. The use of resonators can reduce the thickness required in absorbing layers, and improve modulation contrast [11]. Self-linearized modula-

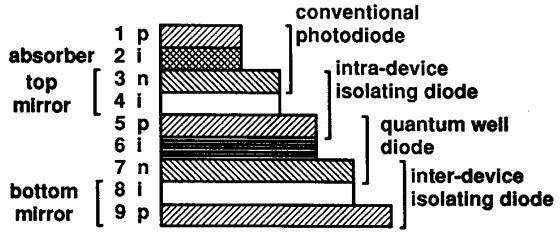

Fig. 7. Layer structure to give conventional and quantum-well photodiodes, together with isolating diodes and with optional mirrors.

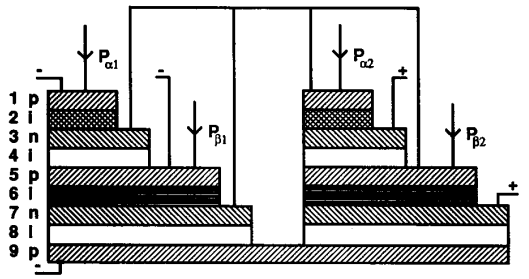

Fig. 8. Illustration of the layer structure and connections to implement the circuit of Fig. 6. The output beams are omitted for clarity, but would either be reflected or transmitted depending on whether a bottom mirror was used.

tors have been demonstrated with such resonator structures [12].

The quantum-well modulator diode is formed from layers 5–7. As usual, it would have transparent p and n regions (e.g., AlGaAs), and a quantum-well *i* region whose thickness would typically be about 1 μm. The circuits require that the conventional diode and the quantum-well diode are electrically isolated from one another. One way to do this would be to grow insulating material between them. This is not always easy, however. An alternative is to use a reverse biased diode to isolate them ("intradevice" isolating diode). To give such a diode a sufficiently large reverse breakdown voltage, it would be desirable to incorporate an intrinsic (*i*) region in the middle. Layers 3–5 form such an "intradevice" isolating diode. When connecting two sets of diodes together to make up circuits, we also need isolation between adjacent quantum-well diodes. One way to do this is to use an insulating substrate or insulating epitaxial layers under the diodes, although again this is not always easy to grow. Another technique, used in many present S-SEED's, is ion implantation [13]. A third technique that also works, and was used in the original S-SEED demonstration [6], is to use the reverse biased diode isolation; such isolation may have the lowest leakage current of all of the techniques, which could be important for analog applications with low light levels. The example structure in Fig. 7 includes such an isolating diode ("interdevice" isolating diode) in layers 7–9. Finally, a dielectric stack mirror may also be incorporated into layers 7–9 to give a reflective device or a resonator structure. The double pass in the reflective device (or the use of the resonator) has the usual advantages of improved contrast ratio or thinner quantum-well region (and hence lower voltage), and allows operation in reflection so that an absorbing substrate (e.g., GaAs) does not have to be removed.

Fig. 8 shows an example set of connections, using the layer structure of Fig. 7, to construct the most complex circuit discussed so far, i.e., the circuit of Fig. 6.

2) *Use of existing S-SEED layer structure:* There are three ways in which we can use a quantum-well diode to substitute for the conventional diode, hence avoiding the necessity of constructing a separate layer structure for the conventional diode. Two of these simply use the same quantum-well diodes simultaneously as the "conventional" and quantum well diodes. The third case uses separate "substitute" quantum-well diodes biased to a higher voltage. All three involve some compromise in performance, although they are all usable.

The first case is when the input light intended for the conventional diodes in the circuits in Figs. 2, 3, 5, and 6 is at a short wavelength. The second case is a small-signal case, where the voltage across the diodes changes little in operation. The most complex circuit, the equivalent of Fig. 6, for these first two cases is shown in Fig. 9.

The first case exploits the fact that the absorption of the quantum-well material is only strongly dependent on voltage near to the optical absorption edge or band-gap wavelength. Although there is some voltage dependence at some shorter wavelengths, at most such wavelengths this is negligible. Hence, at these shorter wavelengths, the quantum-well diode can behave like a conventional photodiode. The best performance would be in the wavelength region where the p and n regions were still transparent, since then all of the incident light would get to the *i*-region for absorption. At short wavelengths, the quantum-well absorption will be stronger, improving the efficiency of conversion of incident photons to current. Such a scheme can be used, for example, for a visible input in beams $P_{\alpha 1}$ and $P_{\alpha 2}$, and the appropriate operating wavelength near the band gap for beams $P_{\beta 1}$ and $P_{\beta 2}$. This is useful for an input device, but the same concept does not work in general when using the output from a previous similar device as the input to this device because the wavelength is wrong.

In the second case, we presume that we are operating with total powers in the two quantum-well diodes that are very nearly equal, i.e., we are making a small-signal assumption, and all beams have the same wavelength. When the total powers incident on the two quantum-well diodes are equal, then the absorption A_0 in both diodes will be equal. From the fact that the same current flows through both diodes in steady state, we know that

$$(P_{\alpha 1} + P_{\beta})A_1 = (P_{\alpha 2} + P_{\beta})A_2 \tag{18}$$

where we have taken the case of equal bias ($P_{\beta 1} = P_{\beta 2} = P_{\beta}$). Now we have, from a simple analysis of the transmission of the two diodes,

$$D_{\text{out}} = P_{\beta}(A_2 - A_1) \tag{19}$$

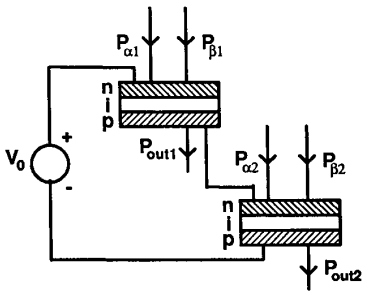

Fig. 9. Version of the circuit of Fig. 6 in which quantum-well diodes substitute for the conventional photodiodes. This involves some compromises in performance, but allows simpler fabrication. It works either for short wavelength input light $P_{\alpha 1}$ and $P_{\alpha 2}$ or for small signal operation (with some loss of input sensitivity).

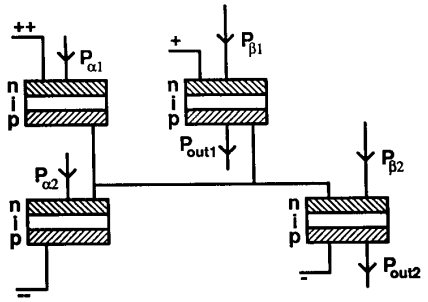

Fig. 10. Version of the circuit of Fig. 6 using separate quantum well diodes to substitute for the conventional photodiodes. In this case, with the substitute quantum-well diodes biased to a higher voltage, the circuit works for large signal operation with some loss of overall sensitivity at the input.

where A_1 and A_2 are the absorptions in the two diodes, respectively. By a simple substitution from (18), we have

$$D_{\text{out}} = \frac{P_\beta A_2}{P_\beta + P_{\alpha 1}} D_\alpha. \tag{20}$$

So far, we have made no approximations. Now we make a small-signal approximation, that $A_2 \cong A_0$ and $P_{\alpha 1} << P_\beta$, and (20) finally becomes

$$D_{\text{out}} \cong A_0 D_\alpha. \tag{21}$$

Hence we have that the difference at the output is proportional to the difference in the input beam powers, although there is now a proportionality constant A_0. We can still use the inputs to sum or difference more than one set of beams, as discussed above, all with the same proportionality constant.

The third case biases the quantum well "substitute" diodes to a higher voltage, as shown in Fig. 10, again for the equivalent of the circuit of Fig. 6. At such high voltages, the quantum-well diode responsivity at the near-band-gap operating wavelength is not strongly dependent on voltage because the absorption edge has been shifted to much longer wavelengths than the desired wavelength for the modulator diodes [14]. Hence the quantum-well diodes behave more like conventional photodiodes. The only compromise is, however, that the absolute absorption in the input photodiodes will not be 100%, and so not all incident photons give rise to electrons. Here also, therefore, we have to derate the difference transferred to the output by a factor A_0, just as in (21). In this case, A_0 is the absorption of the input quantum-well diodes at the high operating bias. The difference between the performance of the circuit of Fig. 10 compared to the performance of the circuit of Fig. 9 is that the circuit of Fig. 10 is not restricted to small signals.

IV. Application Examples for Differential SEED's

To discuss possible applications, it is useful to describe the circuits laid out in a plan view. Fig. 11 shows the nomenclature we will use for this. We will be describing

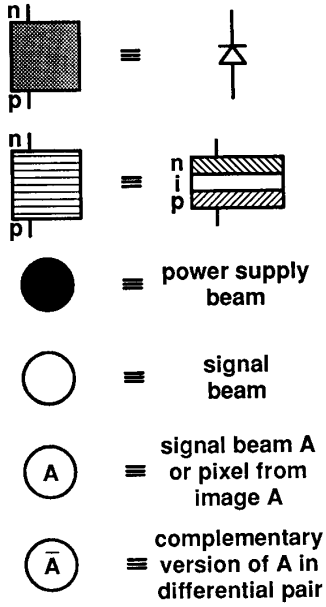

Fig. 11. Nomenclature for plan view circuits. The gray surface represents the top of the conventional photodiode. The surface shown with horizontal lines represents the top of a quantum-well diode.

primarily applications of the circuit of Fig. 6, and the descriptions below will be given for the case using both conventional and quantum-well diodes. Of course, quantum-well diodes may be substituted, as discussed above, with some restrictions. We will not explicitly show the power supply connections for the circuit of Fig. 10, but it will be obvious how to make minor changes to the circuits to accommodate the low and high voltage power supplies.

The circuits will have input beams, which may be either single-ended or differential, usually shining on the conventional diodes. The outputs always come from shining beams through (or reflecting the beams through) the quantum well diodes. The beams that are modulated by the quantum-well diodes will usually be beams all of the same or similar intensities, which we will refer to as power supply beams. These would typically be generated in arrays,

using methods well known from existing digital systems [10]. Some of the example circuits work with pixelated images, whereas others, especially those that evaluate spatial derivatives of an image, are designed to work directly with the original "single ended" image without pixelation.

In the examples here, we will show circuits with differential outputs. In every case, it is also possible to take single ended outputs simply by using the output beam from only one of the two output quantum-well diodes. We discussed the biasing problem of differential-to-single-ended conversion above in Section III-B. In most cases, it is still desirable to illuminate the other quantum-well diode (or a conventional photodiode in effectively the same place in the electrical circuit), because the output will only be able to deal with one sign of electrical current output from the input photodiodes. The illumination of the other diode generates a photocurrent that effectively biases the output so that it can handle both positive and negative inputs. This is especially important when subtracting inputs, since the sign cannot be predicted in advance.

A. Image Addition and Subtraction

Circuits for array elements for addition and subtraction of images are relatively straightforward. Fig. 12 illustrates a simple example of a circuit to subtract the "single-ended" image ***B*** from the "single-ended" image ***A***, giving the result as a differential pair of output beams. The difference between the output beam powers is the difference between the powers in the given pixels of ***A*** and ***B***, regardless of the absolute powers in the input images.

The circuits of Fig. 13 add or subtract images in differential form. Note the difference between the circuits of Fig. 13(b) and (c); in the former, the differential pair is inverted using optics to give the subtraction, whereas in the latter, the inversion is done by rewiring the electrical circuit.

B. Neural Net Node

The circuit of Fig. 13(a) can also function as a node or "neuron" in an optical neural network since it sums all of the input beams. In this case, it is likely that we would wish to extend the number of inputs, which can be done simply by making the conventional photodiode larger. Beams can of course be overlapped on the photodiodes provided that they are not mutually coherent; with mutual coherence, interference can occur which prevents simple summation of powers. Of course we could also use the basic self-linearized modulator structure to sum "single-ended" signals by shining the many inputs to a given "neuron" onto the conventional photodiode. The differential circuit has the advantage that it can handle both positive and negative values at the inputs. These circuits also have a saturating "nonlinear" behavior as desired in many implementations of neural networks. This satura-

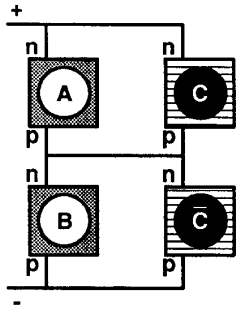

Fig. 12. Circuit to subtract a pixel of image ***B*** from a pixel of image ***A***, given the result as the difference of output powers in the differential pair ***C***.

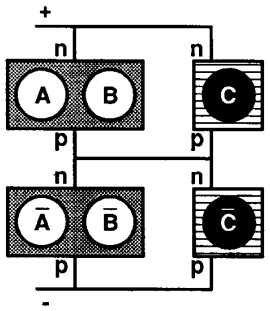

(a)

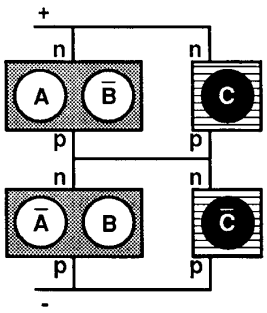

(b)

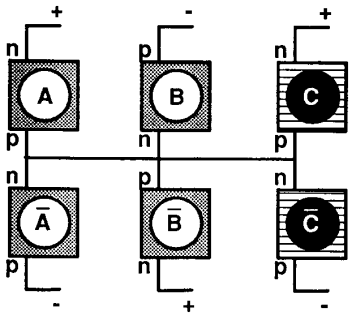

(c)

Fig. 13. Circuits for addition and subtraction of pixels in differential images. (a) Adds two differential images ***A*** and ***B*** giving the result in the differential pair of beams ***C***. (b) and (c) subtract the two differential images, with (b) requiring optical inversion of the beams ***B***, whereas (c) does not because the electrical circuit is rewired to perform the inversion.

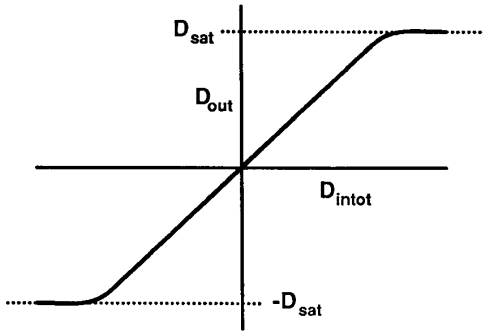

Fig. 14. Illustration of the form of the input/output relationship between the total difference in input powers D_{intot}, to a circuit such as that in Fig. 13(a), and the difference in output powers D_{out}. The output difference saturates at some power D_{sat}.

tion behavior is shown for the differential circuit in Fig. 14.

The difference D_{intot} is the sum of all of the differences in the input beam powers incident on the input conventional photodiodes. D_{out} is the difference in output beam powers. There is a limit to the difference in output beam powers D_{sat} which occurs when an output diode reaches either its minimum or its maximum absorption. The absolute value of D_{sat} depends on the magnitude of the power in the power supply beams. If, for example, the maximum absorption of a diode is 90%, and the minimum absorption is 15%, then the value of D_{sat} will be 75% of the power in a power supply beam. This means that the saturation point of the nonlinearity in Fig. 14 can be controlled optically, and is not set in fabrication. This also means that a network built from such nodes can be tested at low powers, and scaled to high powers.

It might also be of some interest to control the slope of the saturation curve of the neuron. In the simple implementation shown here, the slope is fixed, being essentially 45°. The tangent of the slope could be changed by integer multipliers by using the integer gain or replication discussed below in Sections V and VI. In this case, a unit change in input power difference could produce an integer number of units of change in the output power difference.

C. Optically Controlled Neural Net Multipliers

It is clearly useful in optical neural net systems to be able to control the "synaptic strengths" in the network optically. The synaptic strengths are the multipliers or connection strengths between the output of one neuron and the input of the next. Optical control of these multipliers would mean that the function of the network would not have to be built in during fabrication, and the ability to set all of the multipliers in parallel optically would be a significant feature for optics compared to many other implementations of neural nets. The function performed by such a multiplier is simply that of multiplying one beam or set of beams by another beam or set of beams, and this could also have applications in other optical systems. (It should be noted that this method of making multipliers does not store the value of the multiplier in the circuit, so this is not a useful way of making stored weights for a network that can itself learn.)

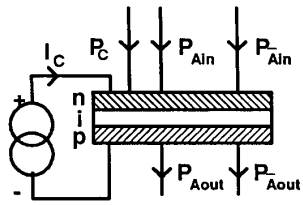

Fig. 15. Circuit for an optically controlled "weight" for an optical neural system. A powerful control beam P_C sets the value of the optical transmission of the signal beam or beams. The figure shows a differential pair of beams being modulated, although the circuit will also work for single beams.

One simple way to make a multiplying factor that can be controlled optically is shown in Fig. 15. This circuit is electrically the same as that of Fig. 1, but adds a further control beam P_C. The simplest way of using this is to have the control beam be much more powerful than the signal beam or beams. Then the amount of absorption in the quantum-well diode is set by the control beam power. The absorbed power in the quantum-well diode is simply given by

$$P_A = P_C A \tag{22}$$

where A is the fractional absorption of the diode. Given that the transmission $T = 1 - A$, then the "multiplier" is, from (4),

$$T = 1 - \frac{\hbar\omega}{e}\frac{I_C}{P_C}. \tag{23}$$

Of course, the values of T are limited by the minimum and maximum transmissions of the quantum-well diode.

In Fig. 15, we show the case where a differential pair of beams P_{Ain} and $P_{\bar{A}in}$ is used to represent the signal being multiplied by the multiplier, with the result being the output beams P_{Aout} and $P_{\bar{A}out}$. The circuit will of course work if only a single beam is used. The differential beam pair has the usual advantage that it can represent positive and negative values of the signal.

The circuit of Fig. 15 still has the limitations that the multiplier T can only be positive, and furthermore is restricted by the range of T allowed by the modulator. In particular, it may be difficult to make $T = 0$ because of the finite contrast ratio of the modulator. Both of these problems are solved by using the circuit of Fig. 16.

This circuit is different from others discussed so far in that it has two quantum-well diodes in series with a current source. We will be discussing other kinds of features of such circuits below. The circuit also requires copies of both input beams; ideally, identical pairs of signal beams land on each diode. The circuit is also straightforward to analyze. For each diode, the same analysis applies as for the circuit in Fig. 15. The most obvious difference in Fig. 16 is that the transmissions of the two diodes are now

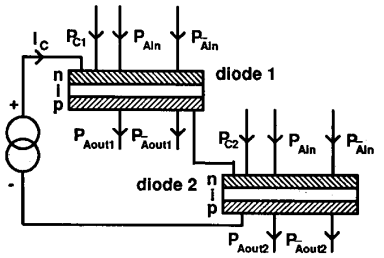

Fig. 16. Multiplier circuit to multiply a differential signal by a positive or negative number. The input differential pair P_A is replicated onto both diodes. The strong powers P_{C1} and P_{C2} control the transmissions of the respective diodes.

independently controllable by the control beams P_{C1} and P_{C2}. To see the full benefits of the circuit of Fig. 16, however, we need to look at beam power differences.

First, we define T_1 and T_2, respectively, as the transmissions of diodes 1 and 2, and

$$D_{A\text{in}} = P_{A\text{in}} - P_{\bar{A}\text{in}} \tag{24}$$

as the difference in the powers in one input beam pair. For the output of this device, we will add the two output differences by adding the powers $P_{A\text{out1}}$ and $P_{A\text{out2}}$ on the input photodiodes of the subsequent neural net node "receiver," to obtain

$$P_{A\text{out}} = P_{A\text{out1}} + P_{A\text{out2}} \tag{25a}$$

and similarly for the other pair $P_{\bar{A}\text{out1}}$ and $P_{\bar{A}\text{out2}}$ to obtain

$$P_{\bar{A}\text{out}} = P_{\bar{A}\text{out1}} + P_{\bar{A}\text{out2}}. \tag{25b}$$

Hence the net difference D_{net} seen by the neural net node receiver is

$$D_{\text{net}} = P_{A\text{out}} - P_{\bar{A}\text{out}} = (T_1 - T_2)D_{A\text{in}}. \tag{26}$$

The "multiplier" now is the *difference* in transmissions $T_1 - T_2$. This can be either positive or negative. Following the same analysis as for (23), we have

$$T_1 - T_2 = \frac{\hbar\omega}{e} I_C \left[\frac{1}{P_{C1}} - \frac{1}{P_{C2}}\right] \tag{27}$$

so that this multiplier is controlled by the powers P_{C1} and P_{C2}. This control could be done by keeping one control beam power fixed and varying the other, although greater dynamic range is possible if both beams are varied.

The scheme of Fig. 16 uses four light beams, and we could refer to this as a "quadriferential" scheme (Latin "*ferre*"—to bear, "*quadri*"—four). As a result of this quadriferential scheme, we are able to perform a full bipolar multiplication of a differential signal. The optics for this is little different from the differential or single-ended schemes. There are several ways in which such circuits could be laid out in plan view, and one example is shown in Fig. 17. The final result D_{net} is given by the difference in optical output powers from the quantum-well diodes. Although only one quadriferential detector layout is shown in Fig. 17(c), in an actual neural application many such receivers might be connected to the same output circuit.

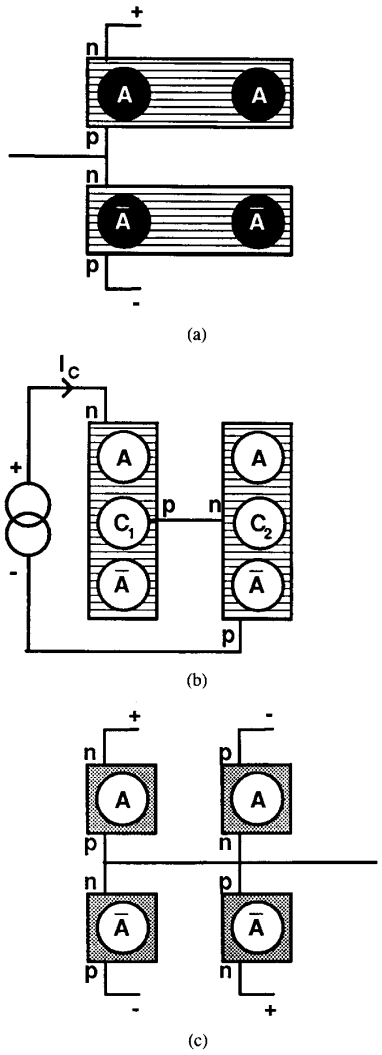

Fig. 17. Circuits for multiplication of a differential signal by a positive or negative number, as for a neural net. (a) Output modulators of the preceding stage; each modulator modulates two identical power beams, all four power beams having equal power. (b) Multiplier, with transmissions of the two quantum-well diodes set separately by the two control beams C_1 and C_2; this is the plan view of the circuit of Fig. 16. (c) "Quadriferential" input detectors for the subsequent stage; these detectors give a current proportional to the difference in the two differential inputs.

D. Evaluation of Spatial Derivatives of an Image

The preceding circuits have dealt mostly with pixelated images; the power of a beam incident on a photodiode may represent the average intensity within the original pixel, although variations in intensity across the beam (i.e., the beam shape) will not in general represent the variations in intensity across the original pixel. Another range of applications is possible that works directly with the unpixelated image to evaluate spatial derivatives. Although the incident image here is not pixelated, the circuits do sample the image and its derivatives. In this case, we imagine that we are shining the image directly onto

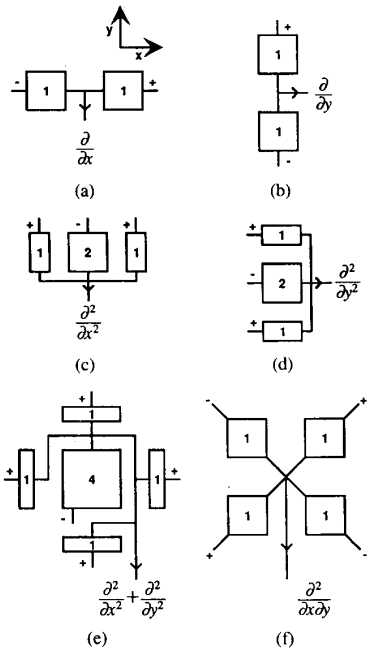

Fig. 18. Various input photodiode layouts for evaluation of local derivatives in a nonpixelated image. For simplicity, shading is omitted on the diodes, and we omit the n and p labels on the photodiode; all diodes are reverse biased. The arrow indicates the current flowing out of the differential detector pair to the output circuit. The value of this current is a direct measure of the derivative. The output circuits themselves are omitted. The numbers on the detectors show the relative photosensitive surface areas of the diodes.

the input photodiodes, and that the intensity varies slowly in space over the size of a photodiode. Now we can use the differential detector scheme to find spatial derivatives.

Fig. 18 shows various layouts of input photodetectors that approximately evaluate various spatial derivatives. These methods of obtaining spatial derivatives by differencing optical powers are essentially the same as those considered by Trabka and Roetling [7] in other implementations. Here we envisage that the detectors are connected in circuits like Figs. 3 or 6. The output quantum-well diodes would be connected to the outputs of the differential detectors, and could give either single-ended or differential outputs. They could be located in the spaces between the input photodiodes, and the necessary power supply beams could be interleaved with the (sampled) input image using the same techniques used to interleave arrays of beams. By this means, we could generate a single-ended or differential array of output beams that represented the local values of the derivatives of the input image. For derivatives, there are strong advantages to the use of the differential outputs, since derivatives can have either sign. Of course, the circuits in Fig. 18 still evaluate the derivatives even if we choose some other output mechanism, and they could drive electrical circuits directly.

The operation of the circuits of Fig. 18(a) and (b) is straightforward; the difference in the powers landing on two equal area diodes space some distance apart is a simple measure of the derivative of the intensity in the direction of separation of the diodes. Fig. 18(c) and (d) can be understood by noting that the second derivative is the difference between two first derivatives separated laterally in space. We could, for example imagine that the large diode in Fig. 18(c) was divided in the middle, with the right half and the rightmost diode forming part a first derivative pair [as in Fig. 18(a)], and the left half and the leftmost diode forming another first derivative pair that is oppositely connected; hence the result is a measure of the second derivative. The circuit of Fig. 18(e) evaluates an approximation to the Laplacian, and can be understood by extension of the arguments for the second derivative circuits. Other layouts of this circuit are possible, including a hexagonal rather than a square layout of diodes, a "picture frame" layout in which the four small diodes are joined to form a continuous frame around the center large diode (with both diodes still having equal area), and a circularly symmetric structure with a center circle and a concentric annular ring, both of equal area. The circularly symmetric version is the best approximation to the Laplacian, but the version of Fig. 18(e) is well suited to a rectangular sampling array, as will be discussed below, and will serve as a useful and nontrivial example in several ways below. The final circuit, Fig. 18(f), evaluates the "cross derivative", and can be understood by a similar analysis.

These kinds of derivative measuring circuits could be useful, especially in arrays, for image processing. The first derivative circuits tend to find edges, especially those of particular orientations. The Laplacian has been used quite generally in early vision processing (see, for example, [15]), and recognizes minima, maxima, and "bumps". The "cross derivative" recognizes saddle points and corners with particular orientations.

As we increase the separation of the diodes in the circuits of Fig. 18, we will generally increase the value of the measured derivative, although we will decrease the spatial resolution. One interesting extension of this is to separate the diodes so much that we interleave them with the diodes of the neighboring elements in an array. This is shown in Fig. 19 for the example of the Laplacian circuit of Fig. 18(e). Now let us presume that the incident image is slowly varying across the diodes within any one dashed circle. To be more precise, the variation of the image intensity within one circle is presumed to be much less than the variation between circles. Now we have a diode layout that evaluates derivatives through finite differences between the values at equally spaced sampling points S_{ij}. This is a more normal sampling scheme for evaluating derivatives. Similar schemes can be devised for the other circuits in Fig. 18.

E. Convolution and Cross Correlation in Real Space

The kind of method shown above in Fig. 19 can be extended to perform a convolution or a cross correlation

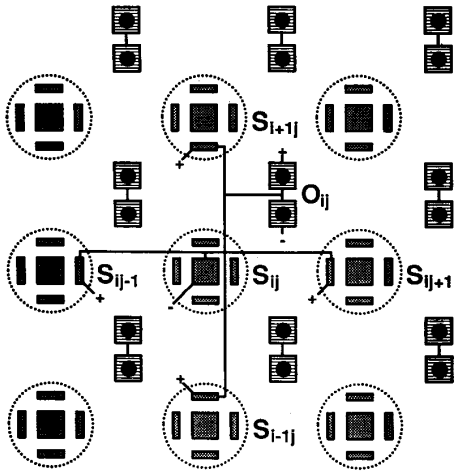

Fig. 19. Diode layout interleaving diodes from adjacent elements in array of circuits as in Fig. 18(c) for evaluating the Laplacian. The input image is shone onto the entire array, for example, through a mask with circular holes corresponding to the sampling circles S_{ij}. Insofar as the intensity within a given circle is approximately uniform, the derivatives evaluated this way correspond to those evaluated approximately by finite differences between sampling points. The outputs are taken from the output diodes O_{ij}. The electrical connections are shown for one set of diodes only for clarity.

in real space, with a fixed kernel. To understand this, we can formally write out the function performed by a circuit such as Fig. 19. In general, we find for the value of the (differential) output O_{ij} from a given quantum-well pair (or alternatively for the net current flowing out of the input photodiodes)

$$O_{ij} = \sum_{k,l} w_{kl} S_{i+kj+l} \tag{28}$$

where the "weights" w_{kl} are the areas of the photodiodes and S_{ij} is the intensity in a given sampling "circle". For the specific Laplacian example of Fig. 19, the relative sizes of the weights are

$$w_{kl} = \begin{Bmatrix} +1, & k = 0 \quad l = \pm 1 \\ -4, & k = l = 0 \\ +1, & k = \pm 1 \quad l = 0 \end{Bmatrix} \tag{29}$$

and zero otherwise.

The process described by (28) is in general a convolution or a cross correlation of the (sampled) image S_{ij} with the kernel w_{kl}. O_{ij} is the convolution of S_{ij} with the kernel w_{-k-l}, and O_{-i-j} is the cross correlation of w_{kl} with S_{ij}. We could construct other kernels of weights, and they could extend over more cells. The weights would still be set by the areas of the photodiodes within each sampling area. As for the simple Laplacian example of Fig. 19, the intensity within each sampling "circle" should not vary by much within the circle for the process to correspond accurately to a convolution or a cross correlation.

As is well known [8], a process such as this can be used to recognize an object, its position, and its amplitude (or "brightness"); the object to be "recognized" is simply related to the pattern w_{kl}. This particular process here will also give the "sign" of the object, i.e., it will detect both positive and negative versions of the desired object, and will say which it is; in other words, the "brightness" or amplitude given by O_{ij} can be positive or negative.

It is interesting to contrast this with the well known Fourier-domain optical processors [8]. Such processors perform correlation or convolution by Fourier transforming the object with a lens, multiplying by a mask in the Fourier plane (since convolution in real space corresponds to multiplication in Fourier space), and inverse Fourier transforming with a second lens to give the result in the output plane. For example, a bright spot will appear in the output plane at points corresponding to the position(s) of the desired object in the input plane. The mask is simply related to the Fourier transform of the desired object. The key difference between the function performed by such processors and the present real-space processor is that the Fourier processors operate on the optical electric field amplitude whereas the present processor operates on the optical intensity. One consequence of this difference is that, as discussed above, the sign of the correlation or convolution shows up directly in the output power difference here, whereas in the Fourier processors it shows up in the sign of the electric field (i.e., its phase), and hence cannot be deduced from the intensity in the output spot alone. (This follows directly from Babinet's principle, since the diffraction pattern of complementary screens is essentially identical except for the sign of the field.) A second difference between the two methods is that it is not necessary to have a coherent source or a coherent version of the image for the present method; we can work directly with a conventional incoherent image as the input without the need for any spatial light modulator to perform incoherent-to-coherent conversion. There is also no need to have mutual coherence between any of the light beams in the system in the present case, so all issues of coherent images, such as speckle, can be avoided.

V. Integer Gain SEED's

If we put several quantum-well diodes in series with a current supply, then in steady state each one is passing exactly the same current; as far as the diodes are concerned, there is no difference between this situation and the situation where, as in Fig. 1, there is only one diode in series with the current supply. We already encountered the case of more than one quantum-well diode in series with a current source for the specific example of the circuit of Fig. 16. Each one of diode 1 and diode 2 is behaving as a self-linearized modulator, independently of the other diode. The only constraints here are that each diode must be operating within its self-linearized range, and the current supply must in practice be capable of providing enough voltage to drive the pair. Hence a current I_C passing through several self-linearized quantum-well diodes in series will result in a power $P_A = (\hbar\omega/e)I_C$ being

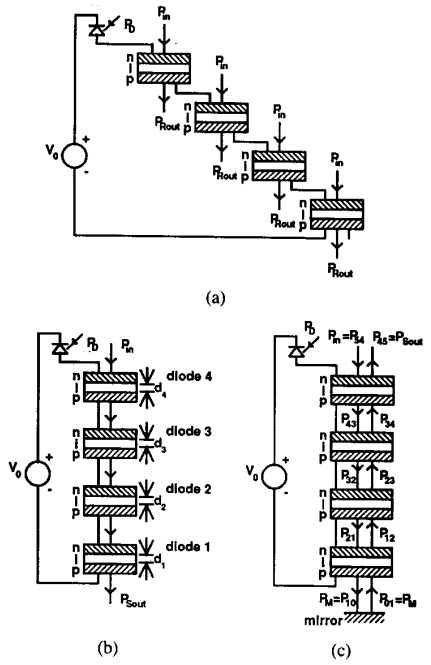

Fig. 20. Multiple self-linearized modulator quantum-well diodes in series with a reverse biased conventional photodiode acting as a constant current source, giving integer optical gain. (a) Replicating SEED, where different beams pass through each of the quantum-well diodes, giving identical output powers P_{Rout} from all four diodes. For each beam $P_{Rout} = P_{in} - P_D$. (b) Transmissive stacked SEED, where the same beam passes though all of the quantum-well diodes, giving an integer gain (in this case, 4) between the incident power P_D and the power $P_{in} - P_{Sout}$ absorbed from the beam P_{in}. (c) Reflective stacked SEED, which also shows integer gain (in this case, 4).

absorbed in *each* diode. This phenomenon can have two kinds of consequences, depending on the optical circuit. Three such optical circuits are illustrated in Fig. 20, where we have used the specific example of a reverse biased conventional "input" photodiode as the current source, and four quantum-well diodes in series.

Following the same analysis as for the simple self-linearized modulator with a photodiode input, the absorbed power in *each* of the quantum-well diodes in Fig. 20 is equal to the incident power P_D shining on the conventional input photodiode. Hence, in all three cases in Fig. 20, the total change in output power [adding all output beams in the case of Fig. 20(a)] is n times the input power P_D, where n is the number of diodes (in this case $n = 4$). All that is required for this integer gain is that the input photodiode absorbs all of the incident power P_A, and that all of the diodes generate one electron of photocurrent for each photon absorbed.

A. Replicating SEED

In Fig. 20(a), the net result of this kind of circuit is to generate n identical output beams. (For simplicity, in Fig. 20(a) we only show the case where the input beams to the four quantum well output diodes are all of equal power, although it is important to realize that, even if these input powers are not equal, the power *absorbed* from each beam is still the same (provided all diodes remain in their self-linearized regimes).) The power subtracted from each of these beams is equal to the power incident on the conventional photodiode, and so we are generating n inverted replicas of the incident beam P_D; hence we can call this circuit a "replicating SEED".

B. Stacked SEED

We can refer to both Fig. 20(b) and (c) as "stacked SEED's". For the case of both Fig. 20(b) and (c), "transmissive" and "reflective" stacked SEEDs respectively, the output power P_{Sout} is given explicitly by

$$P_{Sout} = P_{in} - nP_D \tag{30}$$

hence giving optical signal gain of value n.

The choice of layer thicknesses in the stacked SEED's needs some care. Clearly, for example, if we make the top diode too absorbing, there will not be sufficient power transmitted to the next diode to allow it to generate enough photocurrent. We discuss a specific design procedure for both transmissive and reflective stacked SEED's in the Appendix. This is based on designing for equal field in all diodes at the maximum desired absorption of the whole stack of diodes. Specific designs for a four-diode stacked SEED are given in Table I. The peak absorbance G_m in Table I is equal to $\alpha_{max} d_m$, where α_{max} is the peak absorption coefficient that will be allowed or used at the operating wavelength in the material.

The specific design in Table I illustrates several points. First, in the transmissive version the layers have to become significantly thicker as we move from the input to the output. This is because the power landing on the diodes nearer the output is significantly reduced by the absorption in the preceding diodes, and hence the absorbance must be higher to achieve the same absorbed power. In fact, for the specific design in Table I the layer thickness in diode 1 is becoming very large, and it may be difficult to make such a diode that gives one photoelectron per absorbed photon because of the finite depletion length in real materials. The situation in the reflective case is somewhat different. Here, there is a compensation between the powers in the beams traveling in the two directions through the structure. The "forward" incident power P_{54} on diode 4, for example, is large because it is yet unattenuated, but the "backward" incident power P_{34} is strongly attenuated. Hence the total incident powers on all the diodes tend to be more nearly similar in the reflective case. As a result, the layer thicknesses are more nearly similar in the reflective case. Also, of course, the total absorbing layer thickness in the reflective case is half that required in the transmissive case because the light beam makes two passes through the material.

Figs. 21 and 22 show the results of some designs for reflective stacked SEED's based on the analysis in the Appendix. Fig. 21 shows the designed layer thicknesses for four different cases; these layer thicknesses are ex-

TABLE I
CALCULATED VALUES OF PEAK ABSORBANCES AND LAYER THICKNESSES FOR A STACKED SEED MODULATOR DESIGNED FOR A MINIMUM TRANSMISSION OR REFLECTION OF 0.1, AND ASSUMING A PEAK ABSORPTION COEFFICIENT OF 5000 cm^{-1}.

	Transmissive		Reflective	
Diode Number m	Peak Absorbance G_m	Layer Thickness $d_m(\mu m)$	Peak Absorbance G_m	Layer Thickness $d_m(\mu m)$
1	1.179	2.357	0.349	0.697
2	0.526	1.052	0.313	0.627
3	0.343	0.686	0.266	0.532
4	0.255	0.510	0.223	0.446

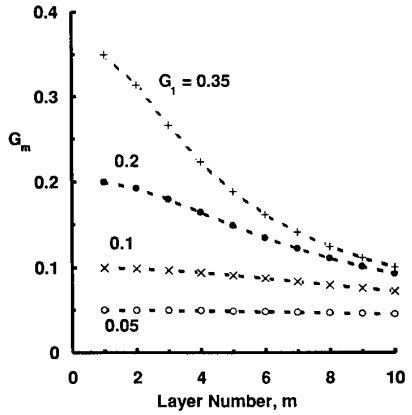

Fig. 21. Peak absorbance G_m (or equivalently absorbing layer thickness expressed in absorption lenghts at the peak absorption coefficient) required in each diode or absorbing layer m of a reflective stacked SEED for each of four different peak absorbances (or layer thicknesses) G_1 in the first layer.

pressed in terms of the peak absorbance $G_m = \alpha_{max} d_m$ of the quantum-well regions in the diodes. Using these layer thicknesses gives the minimum reflectivities R_{min} shown in Fig. 22, for different numbers of diodes in the structure.

C. Physical Structures for Stacked SEED's

The stacked SEED's discussed above could of course be made with many separate quantum-well diodes, or with some optical scheme that passed the same beam sequentially through many series-connected diodes in a planar array. A more convenient alternative would be to grow a "stack" of diodes, one on top of the other. One subtle problem about such structures is that it is easy to make undesired parasitic bipolar transistors out of the various n–p–i–n or p–n–i–p structures that result. Such transistors can introduce gain to various of the layers of the structure; such gain might seem to be desirable for various applications, but it is difficult to control such gain precisely in the fabrication of bipolar transistors. The gain is also dependent on current density in general, and the gain tends to vary with the size of the mesas because of surface recombination. Certainly, to get the precise kind of operation discussed above, we need to suppress the transistor action.

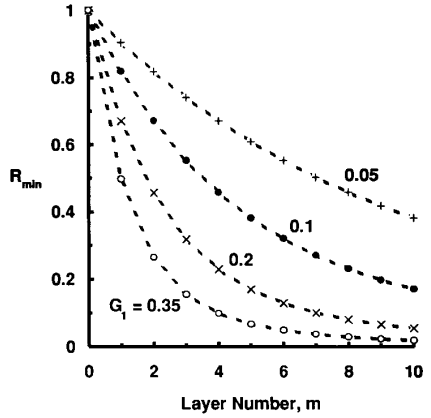

Fig. 22. Minimum reflection R_{min} of a reflective stacked SEED, using the layer thicknesses as shown in Fig. 21, as a function of the number of layers or diodes used, for each of four different choices of peak absorbance G_1 in the first diode.

This same problem of parasitic transistors was solved before in the original integrated diode-based SEED (D-SEED) [16] by growing a tunnel junction between the adjacent diodes. A tunnel junction has the property of "current conversion"; when we flow current through a tunnel junction, hole current flowing on one side of the junction becomes electron current flowing on the other side of the junction (obviously, the electrons and holes flow in opposite directions, but the electrical current flows in the same direction because of the different charges of the electrons and holes). If we put such a junction at the position of the emitter-based junction in a bipolar transistor, we completely prevent normal transistor gain, because we prevent the process of minority carrier injection into the base from the emitter. Technically, we reduce the emitter injection efficiency to zero, giving a transistor with a current gain of unity.

Structures with integral tunnel junctions can be grown, as demonstrated specifically with the integrated D-SEED. There are some technical difficulties with such integral tunnel junctions. It is difficult to make such junctions with high current carrying capacity, and hence the speed of operation of such devices is limited. In the case of the integrated D-SEED, speed was limited to about 1 μs by the maximum tunnel current. Higher maximum tunnel currents require higher doping in the junction; too high a doping can cause morphological problems in the growth, and can result in undesired doping diffusion into other parts of the structure. For slower operating speeds, however, as might be appropriate for real time image processing for example, such junctions appear to be feasible.

Fig. 23 shows an example structure. Here we have put the conventional photodiode on the bottom of the structure; we will shine a pixel of the input image onto it, and the optical power will be absorbed in its i region. The structure of several quantum-well diodes connected through tunnel junctions is on the top of the structure. In the middle is a dielectric stack mirror, designed to reflect

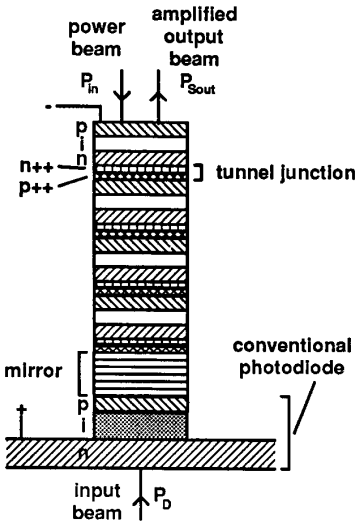

Fig. 23. Structure for a reflective stacked SEED. Here, the input beam P_D is incident on the conventional diode from the bottom, and the power supply beam P_{in} is incident on the stack of four quantum-well diodes from the top. After passing through the stack of quantum-well diodes, being reflected off the dielectric stack mirror, the passing back through the quantum-well diodes, the inverted, amplified output P_{Sout} emerges from the top.

the power beam wavelength. Other structures with such a mirror in the middle have been successfully demonstrated [17]. This structure will produce an inverted version of the input image pixel at the output, amplified by the integer gain of the structure (equal to the number of quantum-well diodes). We can imagine an array of such devices, with an input image on one side, and an amplified output image on the other.

If we use a relatively large number of quantum well diodes in a structure such as Fig. 23, it may also be possible to run the whole device without any electrical power supply; in this case, we may simply connect the top of the quantum-well diode "stack" (the "−"connection in Fig. 23) directly to the bottom of the conventional diode (the "+" connection in Fig. 23). Such "self-biased" SEED's have been demonstrated for bistable operation [18].

The basic principle that allows this self-biased operation to work is the built-in voltage in the diodes. For thin intrinsic regions (as would be appropriate for a high gain device with many diodes), the built-in field can be large enough to give sufficient bias field for the quantum wells, and, as we shine light on the quantum wells, they will start to go into *forward* bias, collectively generating enough *reverse* bias to put the conventional diode into its desired operating region. This would allow an optoelectronic image amplifier with no electrical power supply.

VI. Differential Integer Gain SEED's

We can combine the ideas of the integer gain SEED's and the differential SEED's to make several forms of differential integer gain SEED's. The basic concept here is to take the circuit of Fig. 6, but to replace each output

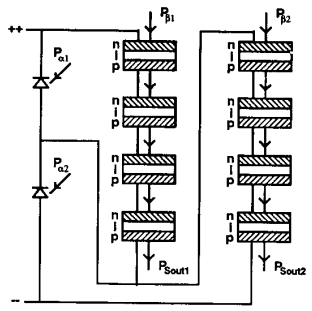

Fig. 24. Differential stacked SEED circuit, analogous to the transmissive stacked SEED circuit of Fig. 20(b). The difference in output power is an amplified version of the difference in input power, with integer gain (in this case, 4).

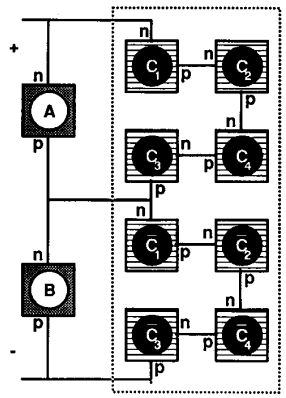

Fig. 25. Differential replicating SEED layout. The difference in any pair of output beams C_i is the difference in the input beam powers A and B. (We assume equal incident powers on all of the output diodes.)

quantum-well diode with a set of quantum-well diodes in series. We can use this to make differential analogs of any of the three circuits of Fig. 20. Fig. 24 shows, for example, a differential transmissive stacked SEED which is the differential analog of the circuit of Fig. 20(b). Fig. 25 shows a plan view of a differential replicating SEED, the differential analog of the circuit of Fig. 20(a).

In these differential cases, incidentally, we can use quantum-well diodes as the input diodes since we can bias them with a larger voltage to make their absorption insensitive to voltage, as discussed above in Section III-C-2. In this case, we may not have complete absorption in the input diode, and hence we will not have strictly integer gain. We will, however, still have equal replicas in the output beams from the different output quantum-well diodes.

A. Differential Stacked SEED

The circuit of Fig. 24 amplifies the difference in the input powers by the integer gain n (here $n = 4$), and presents it as a difference in the output powers. Following the same kind of analysis as used for the circuit of Fig. 6, we obtain

$$D_{Sout} = nD_\alpha + D_\beta \tag{31}$$

where $D_{Sout} = P_{Sout1} - P_{Sout2}$. For $D_\beta = 0$, we have a simple differential amplifier, with differential output. The same analysis would apply to a reflecting stacked SEED. As for the circuit of Fig. 6, we may add or subtract differential signals by shining the differential pairs onto the input conventional diodes, and amplify the result. As (31) shows, we may also add, unamplified, the difference D_β to the output difference.

B. Differential Replicating SEED

In the plan view of Fig. 25, the input beams A and B correspond to the input powers $P_{\alpha 1}$ and $P_{\alpha 2}$ of Fig. 6. The difference between the powers in any pair of output beams, C_i and $\bar{C}_i$ is the same as the input power difference between beams A and B. Clearly we can make analogs of the circuits of Figs. 12 and 13, each with multiple equivalent outputs. This kind of circuit therefore enables us to have a kind of "analog fanout". We will be able to drive the inputs of many circuits with identical analog signals without relying on the accuracy of the splitting ratio of any beamsplitter. The outputs are also separated in space, so we may use simple optical techniques, such as patterned mirrors, to separate the beams and direct them where we wish. Hence we could, for example, use the circuit of Fig. 25 to generate four identical replicas of a pixelated image, separate them optically, and perform four different operations on the image at the same time in the following stage of the processing system.

C. Derivatives and Correlations with Pixelated Images

We discussed above in Section IV how to take derivatives and perform correlations on images that have not been pixelated. The outputs from such circuits are, however, in general pixelated; the outputs are in the form of differential beam pairs spaced throughout the area of the original image. It is not then immediately clear how to perform further such processing on the outputs.

One valid approach to further processing would be to convert back to a single-ended representation by masking off one of the beams in each output pair, and then to perform spatial filtering on the output to remove all of the high frequency components associated with the "sampling" of the output image [8]; this would produce a "smooth" image once more that could be used in further similar processing stages. Such an approach would require more optics, and would throw away some of the power by discarding higher spatial frequency components. Here we propose an alternative method for processing pixelated images (whether from prior processing stages or not); it avoids the additional optics and power loss. The method is suitable for all spatial derivatives, and for correlations with positive or negative integer weights.

The methods for performing these functions rely on the ability to replicate beams. Although it is possible to perform some of these functions with single-ended circuits and representations, we will explicitly discuss only the differential circuits, which have much greater flexibility. The concept is most easily understood by example. In Fig. 26, we are performing the $\partial/\partial x$ horizontal spatial derivative (or, strictly, the difference between adjacent values in the x direction). First, the pixels from the differential input image A are replicated using the circuit of Fig. 26(a) to give the outputs V_{ij}. These outputs are then shone onto the inputs V_{ij} of the circuits in Fig. 26(b). As can be seen by inspection, the differential outputs O_{ij} in Fig. 26(b) give the difference between the differential inputs V_{ij+1} and V_{ij}, hence performing the desired operation. Of course, we could perform this operation without replication on any two adjacent pixels, but the replication allows us to repeat this operation for every pixel in the image, without any need for partially reflecting beamsplitters.

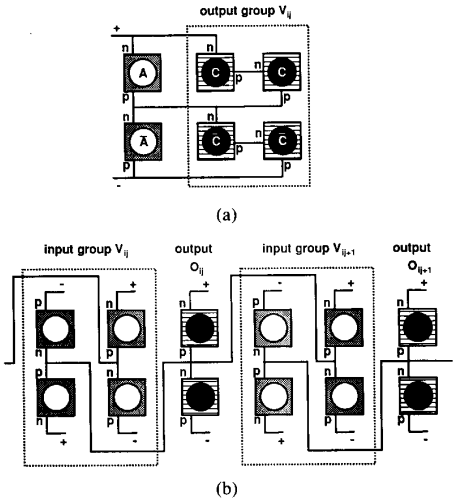

Fig. 26. Illustration of use of replication to perform a horizontal difference (or derivative) on a pixelated differential image. (a) shows the form of the output from the previous stage, with replication into two pairs of output beams V_{ij}. (b) shows the circuit layout to perform the difference operation. The differential output appears at O_{ij}. Full connections are shown for one period of the structure, with illustration of how the connections are continued to successive periods.

The scheme of Fig. 26 can be extended to any kernel with positive or negative integer weights. In Fig. 26, we obtain a negative weight by changing the power supply connections of the photodetectors. To obtain a weight of $\pm m$, we simply arrange for m replicas of the output from the previous stage to land on the same input detector pair. Hence we can perform arbitrary convolutions of pixelated differential images provided that the weights are positive or negative integers. We could in principle handle other weights through the use of attentuators in the beam pairs.

Many of the kernels of interest have the property that the sum of the values of the weights is zero; this is true, for example, for all of the spatial derivative kernels. In a derivative kernel, this zero sum must be true, otherwise a uniform image would give a finite result after convolution with the kernel. It also seems likely that most other kernels designed, for example, for object recognition through

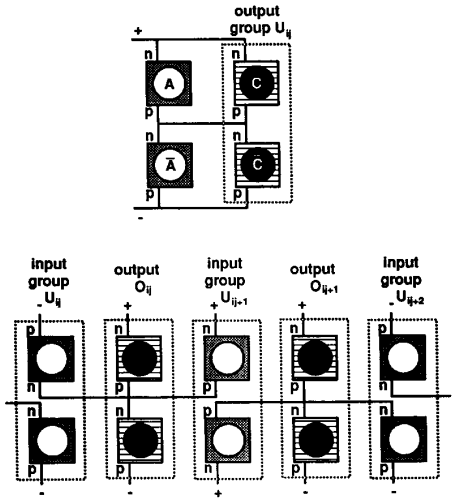

Fig. 27. A simplified version of the circuit of Fig. 26, needing only half of the number of beams. Such a scheme works provided all of the power supply beams on the previous output diodes are equal, and provided that the sum of all the "weights" in the convolution kernel is zero (as it is for all spatial derivative operations).

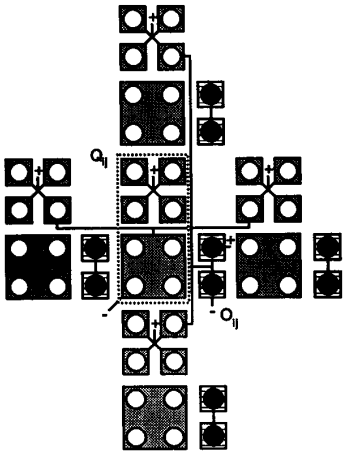

Fig. 28. Diode layout to evaluate an approximation of the Laplacian of a pixelated differential image. The previous stage in the system is presumed to have outputs as in Fig. 25, each consisting of four replicated differential pairs, as shown by the region within the dashed rectangle in Fig. 25. This set of eight beams is incident on the corresponding input diodes within the dashed rectangles in the present figure. The output is given by the differential pairs of quantum well diodes O_{ij}. Electrical connections are shown for one period of the structure only, and p and n markings are omitted for clarity; all diodes are reverse biased.

a convolution/correlation operation, can be cast in this form. Having the object recognition kernels in this "zero-sum" form would seem to be desirable in many cases, since it makes the recognition independent of the degree of background illumination.

When the kernels have this "zero-sum" property (and when all of the elements are positive or negative integers), we can cut the number of output diodes and beams in half. This is illustrated for the very simple example of the horizontal difference operation in Fig. 27. (In this particular, almost trivial, case, there is no need for replication, but in general, the outputs U_{ij} will be replicated.) To use such a circuit, we also require that the powers in all of the power supply beams to all of the output diodes in a previous array be equal.

To have a unit positive weighting from a given output group U_{ij} to a given result O_{kl}, we take an output C and shine it on a "positive" input diode (i.e., one connected to the + supply) connected to the "result" diodes O_{kl}; we could achieve the same result with the complementary output $\overline{C}$ connected to a "negative" input diode (i.e., one connected to the − supply). To achieve a -1 weighting, we would shine a C output on a "negative" diode, or a $\overline{C}$ output on a "positive" diode. We have to have equal amounts of positive and negative weighting, and equal powers in all power supply beams, because we are relying on exact cancellation of the background transmitted power supply "bias" on the positive and negative diodes. In the arrangement of Fig. 26, this cancellation is automatic because it is guaranteed for the diode pair, provided only that the power supply beams were equal within a given beam pair.

A nontrivial example of this "zero-sum" scheme is shown in Fig. 28. Here we are implementing the Laplacian kernel, in analogy to the situation shown in Fig. 19 for nonpixelated images. This is meant to operate with a replicated input like that given by the outputs in Fig. 25.

VII. Physical Performance

The diode circuits discussed here, like many previous SEED circuits, can be used over many others of magnitude in speed and power. The reason for this is that the operating speed is not set by any intrinsic parameter of the devices; the devices change from one state to another by the difference in photocurrents charging the internal capacitance of the devices. The basic methods of analyzing the dynamics of operation of such SEED circuits have been discussed [4]. Running at higher powers gives proportionately higher speeds. At the high speed end, the physical limit on speed is set by absorption saturation and carrier sweep-out times. At the low speed end, the physical limit is set by the leakage current of the devices. Previous SEED's have operated from intensities as low as a few hundred nW/cm^2, with speeds of tens of seconds [5], corresponding to operating energy densities (the product of intensity times time) of the order of 10 $\mu J/cm^2$, to speeds as fast as 33 ps [19] with switching energies of the order of ten picojoules in devices with areas of a few tens of square microns, corresponding to similar operating energy densities. This gives a usable range of as much as 12 orders of magnitude in speed and intensity in this device technology. The full 12 orders of magnitude range would be difficult to attain in one device. The slowest speeds used devices with relatively large mesas; the ratio of surface area to perimeter length would have been relatively large giving a large ratio of capacitance to surface

leakage current, and this would have allowed especially long discharge times. Small devices would likely have faster leakage times. Leakage is also lowest in devices with reverse bias diode isolation between the different parts of the device, and most of the large arrays have used implant isolation instead (to minimize capacitance overall), with a larger leakage current. A usable range of six orders of magnitude is, however, readily possible in one device, and designing for larger ranges (e.g., 9 or 10) seems feasible. The precise energy density required to operate the devices depends on the details of the operating mode and the operating voltage. In practice, the maximum speed is usually set, especially for large arrays, by available optical power.

A. Formal Analysis

The dynamics of self-linearized operation have not been explicitly discussed before. A full discussion of the physical performance of these devices is beyond the present paper; the current in the photodiodes is not accurately linear in voltage, and hence a full understanding of the dynamic response would require simulations. We can, however, understand the main features from a simple linearized analysis. The necessary equivalent circuit is shown in Fig. 29.

In Fig. 29, I_c is the drive current, which could be from a photodiode or the differential current from a pair of photodetectors. $I_A(V)$ is the photocurrent from the absorption in the quantum-well output diode as a function of the voltage V across the diode; equivalently, $I(V)$ could be the difference in photocurrents in a pair of quantum-well diodes, with V then being the voltage across one diode. C is the total capacitance of all the diodes, including any relevant stray capacitance. We will explicitly discuss the simple case corresponding to the circuit of Fig. 1. We know from Fig. 29 that

$$\frac{dV}{dt} = \frac{I_C - I_A(V)}{C}. \tag{32}$$

We presume that we are operating in the vicinity of some "equilibrium" voltage V_{eq}, at which $I_c = I_A(V_{eq})$, and about which the absorption A of the quantum-well diode changes approximately linearly with voltage, i.e.,

$$A \cong A_{eq} + \gamma(V - V_{eq}) \tag{33}$$

where

$$\gamma = \left.\frac{dA}{dV}\right|_{V_{eq}}. \tag{34}$$

Since $I_A(V) = (e/\hbar\omega)P_{\text{in}}A(V)$, where P_{in} is the input optical power on the quantum-well diode, simple algebra shows that the voltage settles towards "equilibrium" with an exponential decay time constant

$$\tau = \frac{\hbar\omega}{e}\frac{C}{\gamma P_{\text{in}}}. \tag{35}$$

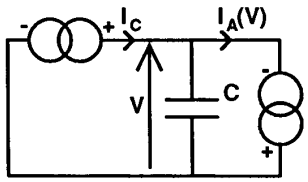

Fig. 29. Equivalent circuit for analyzing the dynamic response of the self-linearized modulators.

τ is the characteristic response time of the self-linearized system, at least for small signal behavior. Equation (35) shows, as we would expect, that larger capacitance gives slower response, and larger incident power P_{in} and larger modulator sensitivity γ give faster response.

If we repeat this analysis for the case of the self-linearized differential modulator (e.g., the circuit of Figs. 4 or 6), the time constant is halved compared to (35) if we put power P_{in} into each quantum well diode. In the differential case, it is the difference in the two photocurrents in the quantum-well diodes that charges the capacitance; this is larger by a factor of two compared to the single-ended case because one diode decreases absorption as the other increases. In fact, however, this factor of two improvement will likely be canceled out by the doubling of the capacitance in the differential case because of the doubling of the number of diodes. Hence the times for the two cases are identical for identical diode designs and identical powers on the diodes. We will therefore only do the calculation for the single ended case, but the results apply to both single-ended and differential circuits.

For the case of the integer gain SEED's, the current sources for the analysis are identical, but the voltage swing is magnified by a factor of n for a given γ, where n is the number of series quantum-well diodes in a set. As a result, the formula (35) for τ becomes multiplied by an additional factor of n. The capacitance C is the capacitance seen from the point where the conventional and quantum-well diodes are connected.

For the case of the replicating SEED, we can presume that the quantum-well diode design is the same as we would have for the simple single (i.e., $n = 1$) quantum-well diode case. Hence, the capacitance from the quantum-well diodes is reduced by a factor $1/n$, because there are n diodes in series. However, the capacitance from the conventional diodes is likely to be unchanged; because this contribution to the capacitance does not reduce by a factor n, it is likely to dominate, and the additional factor of n in τ will not be canceled. Consequently, the replicating SEED is likely to run of the order of n times slower than the related circuit with $n = 1$ (i.e., only one quantum-well diode per set).

In the case of the stacked SEED, the individual quantum well diodes will be of the order of $1/n$th as thick as a single diode would be (especially in the reflective case); as a result, the capacitance of an individual diode will be of the order of n times larger, although the set of n series diodes will end up by having approximately the same total

(series) capacitance as the case with $n = 1$. γ (the change in absorption per unit voltage on a given diode) will be approximately the same size in the thin diodes as it would have been in the single diode; although the diode is $1/n$th as absorbing, it is n times more sensitive to voltage. Hence in the stacked SEED also there is no real cancelation of the factor of n in τ, and the stacked SEED will also run n times slower than the related circuit with $n = 1$. Hence, in both of the integer gain SEED's we see a constant gain-bandwidth product.

There are, incidentally, several methods we could use to get power gain with these devices. We could, for example, use avalanche gain in the input photodiodes. If we were interested only in binary output, we could use the methods already used with *S*-SEED's in digital systems [6]. There we shine a pair of shorter wavelength "clock" beams on a differential pair to force the diode into a bistable state; the state chosen reflects the sign of the current into the center of the pair. Such a binary output can be read out at arbitrarily high power (time-sequential gain).

B. Calculated Performance

We can calculate some representative values for the performance of simple circuits. The typical value of C is about 10^{-16} F/μm^2 for diodes with about 1 μm thick intrinsic regions. γ can be about 0.03 to 0.1 V^{-1} in typical modulators. As an example for a simple self-linearized modulator with 10×10 μm^2 conventional and quantum-well diodes, the capacitance might be about 30 fF (for a single-ended circuit) allowing for some stray capacitance. At about 850 nm wavelength (about 1.5 eV photon energy), we would have response times τ of the order of 1.5–5 ns for $P_{in} = 300$ μW; this is a power level that can be handled by such diodes, as has been demonstrated in digital applications. For a response time of 10 ms, as might be appropriate for analog optical processing in video applications, the input power levels for the quantum well diodes would be about 50–150 pW; in this case, input intensities of about 50–150 μW/cm^2 on the conventional diode (corresponding to 50–150 pW in the 10×10 μm^2 diode area) would be sufficient to achieve the maximum possible modulation of the output. Hence we can expect useful modulation (i.e., many percent) at video rates with input image intensities in the range of a few μW/cm^2. These intensities are comparable to the intensities in the image plane of a typical camera lens when viewing in normal room lighting; hence these devices may allow processing at video rates directly with ambient illumination of an input object imaged onto the array with conventional optics. Present SEED technology with such diode circuits can successfully fabricate arrays of about 10 000 elements with quantum-well diodes of these dimensions. The total of the optical powers P_{in} required to run an array of 10 000 such devices at this speed would be only 1 μW. Such a power could be generated, for example, by one light emitting diode, with some spectral filtering to select the desired wavelength. The electrical current required for the whole array would be the order of 1 μA.

VIII. Conclusion

We have proposed a new set of circuits and operating modes for quantum-well self-electrooptic-effect devices. These proposed devices can operate linearly to add, substract, replicate, and differentiate analog optical signals, and multiply the signals by integer gains. Such integer gain would allow, for example, uniform amplification of an image. The devices are compatible with existing semiconductor technology for 2-D arrays, and many of the devices could be made using the existing process for symmetric SEED's. Arrays can operate on whole images at once, and can convolute and cross correlate with fixed patterns. We have also shown circuits that allow optically controlled bipolar multiplication weights for matrix-vector multiplication or optical neural nets.

Although many of these devices can work with conventional single-ended optical signals, there are versions of all of them that work with differential pairs of light beams. The use of differential pairs allows positive and negative values to be represented, as required, for example, in image differences and spatial derivatives. Circuits are also given for conversion between differential and signal-ended representations. These circuits may therefore allow full bipolar optical processing without the need for coherent light. The differential representation is also practically convenient because it makes the devices insensitive to the absolute optical supply power and to overall variations in supply power across an array, and allows the use of modulators with modest contrast ratios. Many of these concepts of differential representation may extend beyond these specific devices.

The devices described here have a wide potential operating speed range, and have low operating energies. For example, operation as fast as a few nanaoseconds is expected at operating powers of hundreds of microwatts per device with 10×10 μm devices. Speeds as slow as seconds may be possible with proportionately lower intensities. It should also be possible to form an image on the devices of a scene under normal room illumination, and process it directly at video frame rates.

These proposed devices therefore offer many new possibilities for optical analog processing systems.

Appendix
Design of Stacked SEED's

A way of approaching the design of stacked SEED's is to choose layer thicknesses so that a particular absorption coefficient all diodes have the same absorption. The absorption coefficient (at a given wavelength) is only a function of the field. Hence, with this design approach, there is a set of conditions for which the field is the same in all diodes. We could reasonably choose this absorption coefficient to be the largest one we intend to allow, α_{max}, which will also correspond to the largest field we intend

to allow since we want to stay in the regime where absorption coefficient increases with field. This is not the only approach we could take, but it is a reasonable one, and minimizes the total thickness of absorbing material we require to achieve a given minimum transmission or reflectivity.

Transmissive Stacked SEED

For the "straight through" transmissive stacked SEED [Fig. 20(b)], we may start by choosing the number of diodes n (i.e., the desired gain), and the desired minimum total transmission T_{min}, of the stacked SEED. Of course, at all times when the diodes are in their self-linearized region, the power in each diode is the same, and is equal to P_D. We know, therefore, that the total power absorbed by the quantum-well diodes is nP_D, since P_D must be absorbed in each, and hence, for the specific minimum transmission case

$$n\frac{P_{Dmax}}{P_{\text{in}}} = (1 - T_{min}) \tag{A1}$$

where P_{Dmax} is the incident power on the conventional diode that will lead to the minimum transmission being reached for a given T_{min}. In fact, (A1) defines P_{Dmax} for given n, T_{min} and P_{in}.

For any layer m with incident power P_{inm}, we can readily deduce that the thickness of the layer should be

$$d_m = \frac{-1}{\alpha_{max}} \log\left(1 - \frac{P_{Dmax}}{P_{\text{in}m}}\right) \tag{A2}$$

so that it absorbs a power P_{Dmax}. But

$$P_{\text{in}m} = P_{\text{in}} - (n - m)P_{Dmax} \tag{A3}$$

since power P_{Dmax} is absorbed in each layer. Substituting from (A1) in (A3) and finally in (A2), we obtain

$$d_m = \frac{1}{\alpha_{max}} \log\left(\frac{n - (n - m)(1 - T_{min})}{n - (n - m + 1)(1 - T_{min})}\right) \tag{A4}$$

which gives the desired thicknesses of the layers.

Reflective Stacked SEED

The analysis of the reflecting stacked SEED is somewhat more complex. Specifically, we cannot simply work from the input P_{in} to the output $P_{S\text{out}}$ because the power absorbed in a given quantum-well diode is the sum of the power absorbed from both the forward and backward beams. We can, however, analyze the circuit by starting from the mirror and working upwards through the diodes. In this case, once we choose an absorbance, $D_1 = \alpha_{max}d_1$, for the bottom (i.e., first) diode, we can deduce all of the absorption thicknesses for the other diodes, and finally deduce R_{min}, the minimum reflectivity. (Choosing $\alpha_{max}d_1$ is equivalent to choosing P_{Dmax}/P_M.)

We can readily calculate the absorbed power in any diode based on the powers incident on the diode. This absorbed power is always equal to P_D when the quantum-well diodes are all in their self-linearized region, so we have for the maximum absorption case

$$P_{Dmax} = (P_{m+1m} + P_{m-1m})(1 - e^{\alpha_{max}d_m}). \tag{A5}$$

(The notation P_{pq} refers to the power from the pth diode landing on the qth diode.) It is more convenient to write this in terms of the powers on the "lower" side of the diode since we will be working step by step from the bottom of the stack. Since

$$P_{mm+1} = P_{m+1m}e^{-\alpha_{max}d_m} \tag{A6}$$

we have, from (A5),

$$P_{Dmax} = (P_{mm-1}e^{\alpha_{max}d_m} + P_{m-1m})(1 - e^{-\alpha_{max}d_m}). \tag{A7}$$

Equation (A7) is a quadratic equation for $e^{-\alpha_{max}d_m}$, which we can solve to give the layer thickness d_m in terms of the powers below layer m,

$$d_m = \frac{1}{\alpha_{max}} \log\left[2P_{m-1m}\left((P_{Dmax} + P_{mm-1} - P_{m-1m}) \cdot \left\{\sqrt{1 + \frac{4P_{m-1m}P_{mm-1}}{(P_{Dmax} + P_{mm-1} - P_{m-1m})^2}} - 1\right\}\right)^{-1}\right]. \tag{A8}$$

Now we may proceed to solve from the bottom of the structure. We start by choosing $\alpha_{max}d_1$ (and P_M, although this is only a scale factor of no real importance). We know that $P_{10} = P_{01} = P_M$, since we presume that the mirror reflectivity is 100% (other reflectivities could readily be handled here if desired). We then deduce P_{Dmax} from (A5) for layer 1. Then we use (A6) and the similar equation

$$P_{mm+1} = P_{m-1m}e^{-\alpha_{max}d_m} \tag{A9}$$

to deduce the powers above diode 1 as input to (A8) for layer 2, and so on. When we have completed this process for all of the layers, we know all of the layer thicknesses, and we know the input power P_{in} and the output power $P_{S\text{out}}$ at the maximum absorption condition, i.e., we know R_{min}. Results for the layer thicknesses and minimum reflectivities for various $\alpha_{\max}d_1$ are shown in Figs. 21 and 22, respectively.

References

[1] D. A. B. Miller, "Quantum well self-electro-optic effect devices," *Opt. Quantum Electron*, vol. 22, pp. S61-S98, 1990.

[2] A. L. Lentine and D. A. B. Miller, "Evolution of SEED technology: Bistable logic gates to optoelectronic smart pixels," *IEEE J. Quantum Electron.*, this issue, pp. 655-669.

[3] D. A. B. Miller, D. S. Chemla, T. C. Damen, A. C. Gossard, W. Wiegmann, T. H. Wood, and C. A. Burrus, "Electric field dependence of optical absorption near the bandgap of quantum well structures," *Phys. Rev. B*, vol. 32, pp. 1043-1060, 1985.

[4] D. A. B. Miller, D. S. Chemla, T. C. Damen, T. H. Wood, C. A. Burrus, A. C. Gossard, and W. Wiegmann, "The quantum well self-electrooptic effect device: Optoelectronic bistability and oscillation, and self linearized modulation," *IEEE J. Quantum Electron.*, vol. QE-21, pp. 1462-1476, 1985.

[5] G. Livescu, D. A. B. Miller, J. E. Henry, A. C. Gosssard, and J. H. English, "Spatial light modulator and optical dynamic memory using a 6 × 6 array of self-electro-optic-effect devices," *Opt. Lett.*, vol. 13, pp. 297-299, 1988.

[6] A. L. Lentine, H. S. Hinton, D. A. B. Miller, J. E. Henry, J. E. Cunningham, and L. M. F. Chirovsky, "Symmetric self-electrooptic effect device: Optical set-reset latch, differential logic gate, and differential modulator detector," *IEEE J. Quantum Electron.*, vol. 25, pp. 1928-1936, 1989.

[7] E. A. Trabka and P. G. Roetling, "Image transformations for pattern recognition using incoherent illumination and bipolar aperture masks," *J. Opt. Soc. Amer.*, vol. 54, pp. 1242-1252, 1964.

[8] J. W. Goodman, *Introduction to Fourier Optics.* New York: McGraw-Hill, 1968.

[9] S.-K. Kwong, G. A. Rakuljic, V. Leyva, and A. Yariv, "Real-time image processing using a self-pumped phase conjugate mirror," *Proc. SPIE*, vol. 613, p. 36, 1986.

[10] N. Streibl, K. H. Brenner, A. Huang, J. Jahns, J. Jewell, A. W. Lohmann, D. A. B. Miller, M. Murdocca, M. E. Prise, T. Sizer, "Digital optics," *Proc. IEEE*, vol. 77, pp. 1954-1969, 1989.

[11] M. Whitehead, A. Rivers, G. Parry, and J. S. Roberts, "Very low voltage, normally-off asymmetric Fabry-Perot reflection modulator," *Electron. Lett.*, vol. 26, pp. 1588-1590, 1990.

[12] B. L. Shoop, B. Pezeshki, J. W. Goodman, and J. S. Harris, "Noninterferometric optical subtraction using reflection-electroabsorption modulators," *Opt. Lett.*, vol. 17, pp. 58-60, 1992.

[13] A. L. Lentine, F. B. McCormick, R. A. Novotny, L. M. F. Chirovsky, L. A. D'Asaro, R. F. Kopf, J. M. Kuo, and G. D. Boyd, "A 2 kbit array of symmetric self-electrooptic effect devices," *IEEE Photon. Technol. Lett.*, vol. 2, pp. 51-53, 1990.

[14] See for example absorption data in A. M. Fox, D. A. B. Miller, G. Livescu, J. E. Cunningham, and W. Y. Jan, "Quantum well carrier sweep out: Relation to electroabsorption and exciton saturation," *IEEE J. Quantum Electron*, vol. 27, pp. 2281-2295, 1991.

[15] C. Mead, *Analog VLSI and Neural Systems.* New York: Addison-Wesley, 1989.

[16] D. A. B. Miller, J. E. Henry, A. C. Gossard, and J. H. English, "Integrated quantum well self-electro-optic effect device: 2×2 array of optically bistable switches," *Appl. Phys. Lett.*, vol. 49, pp. 821-823, 1986.

[17] S. Matsuo, C. Amano, and T. Kurokawa, "Photonic memory switch consisting of multiple quantum well reflection modulator and heterojunction phototransistor," *Appl. Phys. Lett.*, vol. 60, pp. 1547-1549, 1992.

[18] K. W. Goossen, J. E. Cunningham, D. A. B. Miller, W. Y. Jan, A. L. Lentine, A. M. Fox, and N. K. Ailawadi, "Low field electroabsorption and self-biased self-electro-optic effect device using slightly asymmetric coupled quantum wells," in *Quantum Optoelectronics, 1991, Tech. Dig. Ser.*, vol. 7. Wash,. DC: OSA, 1991, pp. 26-29.

[19] G. D. Boyd, A. M. Fox, D. A. B. Miller, L. M. F. Chirovsky, L. A. D'Asaro, J. M. Kuo, R. F. Kopf, and A. L. Lentine, "33 ps optical switching of symmetric self-eletro-optic effect devices," *Appl. Phys. Lett.*, vol. 57, pp. 1843-1845, 1990.

David A. B. Miller (M'84-SM'89), for a photograph and biography, see this issue, p. 669.